BRAIN COMMUNICATIONS

The adult human subventricular zone: partial ependymal coverage and proliferative capacity of cerebrospinal fluid

Sophia F. A. M. de Sonnaville,[1,2,*] Miriam E. van Strien,[1,*] Jinte Middeldorp,[1] Jacqueline A. Sluijs,[1] Simone A. van den Berge,[3] Martina Moeton,[3] Vanessa Donega,[1] Annemiek van Berkel,[1] Tasmin Deering,[1] Lidia De Filippis,[4] Angelo L. Vescovi,[4] Eleonora Aronica,[5,6] Rainer Glass,[7] Wilma D. J. van de Berg,[8] Dick F. Swaab,[9] Pierre A. Robe[2,**] and Elly M. Hol[1,3,**]

* These authors contributed equally to this study.

** These authors share senior authorship.

Neurogenesis continues throughout adulthood in specialized regions of the brain. One of these regions is the subventricular zone. During brain development, neurogenesis is regulated by a complex interplay of intrinsic and extrinsic cues that control stem-cell survival, renewal and cell lineage specification. Cerebrospinal fluid (CSF) is an integral part of the neurogenic niche in development as it is in direct contact with radial glial cells, and it is important in regulating proliferation and migration. Yet, the effect of CSF on neural stem cells in the subventricular zone of the adult human brain is unknown. We hypothesized a persistent stimulating effect of ventricular CSF on neural stem cells in adulthood, based on the literature, describing bulging accumulations of subventricular cells where CSF is in direct contact with the subventricular zone. Here, we show by immunohistochemistry on *post-mortem* adult human subventricular zone sections that neural stem cells are in close contact with CSF via protrusions through both intact and incomplete ependymal layers. We are the first to systematically quantify subventricular glial nodules denuded of ependyma and consisting of proliferating neural stem and progenitor cells, and showed that they are present from foetal age until adulthood. Neurosphere, cell motility and differentiation assays as well as analyses of RNA expression were used to assess the effects of CSF of adult humans on primary neural stem cells and a human immortalized neural stem cell line. We show that human ventricular CSF increases proliferation and decreases motility of neural stem cells. Our results also indicate that adult CSF pushes neural stem cells from a relative quiescent to a more active state and promotes neuronal over astrocytic lineage differentiation. Thus, CSF continues to stimulate neural stem cells throughout aging.

1 Department of Translational Neuroscience, UMC Utrecht Brain Centre, University Medical Centre Utrecht, University Utrecht, Utrecht, The Netherlands
2 Department of Neurosurgery, UMC Utrecht Brain Centre, University Medical Centre Utrecht, University Utrecht, Utrecht, The Netherlands
3 Department of Neuroimmunology, Netherlands Institute for Neuroscience, An Institute of the Royal Netherlands Academy of Arts and Sciences, Amsterdam, The Netherlands
4 Department of Regenerative Medicine, IRCCS Casa Sollievo della Sofferenza, San Giovanni Rotondo, Italy
5 Department of (Neuro)pathology, Amsterdam University Medical Centre, University of Amsterdam, Amsterdam, The Netherlands
6 Stichting Epilepsie Instellingen Nederland (SEIN), Heemstede, The Netherlands
7 Department of Neurosurgical Research, Clinic for Neurosurgery, Ludwig Maximilian University of Munich, Munich, Germany

Received January 29, 2020. Revised July 30, 2020. Accepted August 4, 2020. Advance Access publication October 13, 2020

8 Department of Anatomy and Neurosciences, Section Clinical Neuroanatomy, Amsterdam University Medical Centre, Location VU, Amsterdam, The Netherlands
9 Department of Neuropsychiatric Disorders, Netherlands Institute for Neuroscience, An Institute of the Royal Netherlands Academy of Arts and Sciences, Amsterdam, The Netherlands

Correspondence to: Elly M. Hol, PhD
Department of Translational Neuroscience
UMC Utrecht Brain Centre, University Medical Centre Utrecht
Internal postal address Str. 4.205/P.O. Box 85060
Utrecht, The Netherlands.
E-mail: e.m.hol-2@umcutrecht.nl

Keywords: cerebrospinal fluid; glial nodules; human; neural stem cells; subventricular zone

Abbreviations: ASCL1 = achaete-scute family bHLH transcription factor 1; BSA = bovine serum albumin; DAB = 3,3'-diaminobezidine tetrahydrochloride; DCX = doublecortin; DMEM = Dulbecco's modified Eagle's medium; EF1α = elongation factor 1-alpha; EGF(R) = epidermal growth factor (receptor); FGF(R) = fibroblast growth factor receptor; FOXJ1 = forkhead box protein J1; FCS = foetal calf serum; GAPDH = glyceraldehyde-3-phosphate dehydrogenase; GFAP = glial fibrillary acidic protein; GLUL = glutamate-ammonia ligase; HES = hes family bHLH transcription factor; HLA-DR = human leucocyte antigen – DR isotype; JAG1 = jagged canonical Notch ligand 1; NBB = Netherlands Brain Bank; NCAM1 = neural cell adhesion molecule 1; NDC = non-demented control; NES = nestin; NOTCH1 = notch receptor 1; NPC = neural progenitor cell; NSC = neural stem cell; PCNA = proliferating cell nuclear antigen; PMD = *post-mortem* delay; P/S = penicillin/streptomycin; PSEN1 = presenilin 1; S100β = S100 calcium-binding protein B; SGN = subventricular glial nodule; SLC1A2 = Solute carrier family 1 member 2; SOX2 = Sex determining region box 2; SVZ = subventricular zone; TBS = Tris-buffered saline; TUBB = tubulin; VIM = vimentin

Graphical Abstract

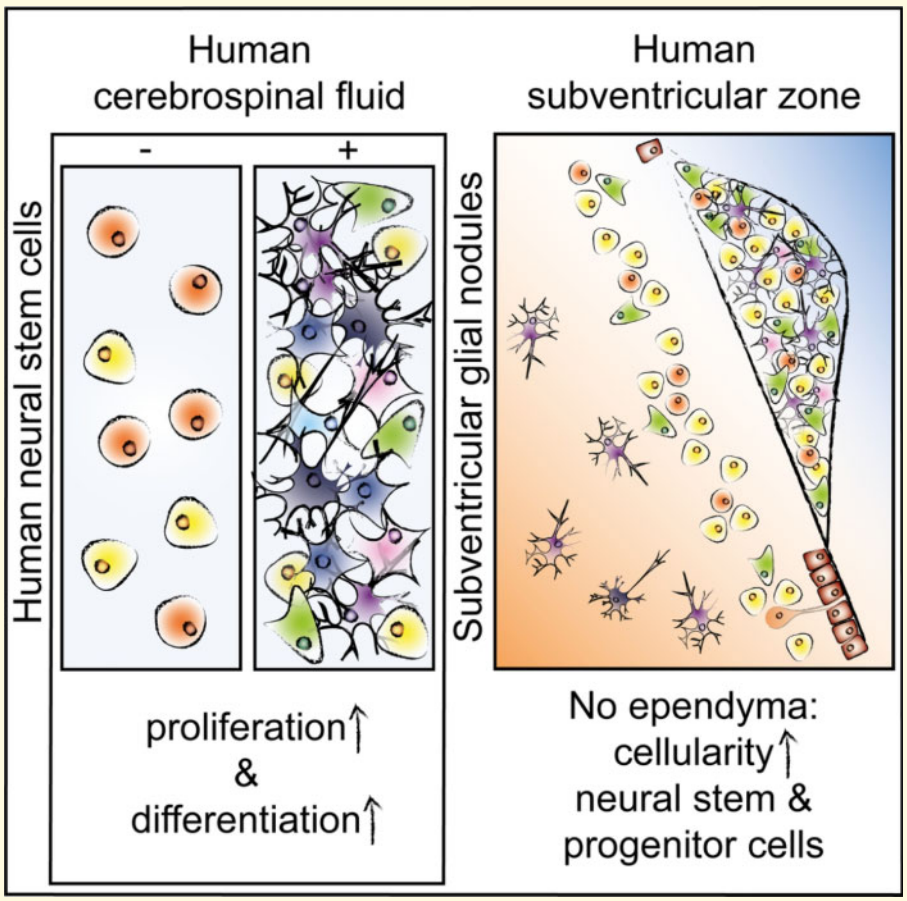

Introduction

The subventricular zone (SVZ) is a neurogenic brain area that lines the walls of the ventricles. Subventricular zone neural stem cells (NSCs) are able to proliferate and differentiate into neurons and glial cells (Doetsch *et al.*, 1999; Kukekov *et al.*, 1999; Sanai *et al.*, 2004). During brain development, radial glia are in direct contact with cerebrospinal fluid (CSF), which provides important growth factors and cues for directional migration (Sawamoto, 2006; Johansson *et al.*, 2010; Zappaterra and Lehtinen, 2012; Ortega *et al.*, 2018). In rodents, NSCs are in direct contact with CSF through apical processes (Mirzadeh *et al.*, 2008). In humans, adult NSCs are arranged in a ribbon, which is separated from the CSF by a single layer of ependymocytes and a hypocellular gap (Sanai *et al.*, 2004; van den Berge *et al.*, 2010; Jiménez *et al.*, 2014). Human NSC protrusions extend through the ependymal cell layer towards the ventricle as shown by Sanai *et al.* (2004). The ependyma forms a semi-permeable CSF–brain barrier supported by incomplete apical tight junctions, lateral adherens and gap junctions, a luminal sialic acid coating and aquaporin-4 channels on the basolateral membrane (Nielsen *et al.*, 1997; Schauer, 2009; Zhang *et al.*, 2010; Lehtinen and Walsh, 2011; Jiménez *et al.*, 2014). At young age, this barrier is largely intact; however, increased penetrance of CSF into the parenchyma has been described in aged rodents (Whish *et al.*, 2015), and some ependymal loss has been shown in human adults (Del Bigio, 2010). The effect of increased direct contact of NSCs with CSF in the adult human SVZ is largely unknown.

Cerebrospinal fluid is primarily produced by the choroid plexus (Oreković and Klarica, 2010), and contains a broad spectrum of proteins including growth factors that are key for neurogenic signalling (for a review, see Zappaterra and Lehtinen, 2012). The few studies applying rodent and, in some cases, human-derived CSF to neural stem and progenitor cells mainly suggest that CSF enhances survival and stimulates proliferation of NSCs, but the effect is controversial. In addition, from these studies the effect of CSF on stem cell differentiation and migration remains unclear (Gato *et al.*, 2005; Buddensiek *et al.*, 2009, 2010; Lehtinen *et al.*, 2011; Ma *et al.*, 2013; Zhu *et al.*, 2015; Alonso *et al.*, 2017). Human CSF composition changes with age (Zhang *et al.*, 2005; Baird *et al.*, 2012), with a concomitant decrease in NSC number in the SVZ and a significant reduction of the rostral migratory stream (Sanai *et al.*, 2005, 2011; Conover and Shook, 2011; van Strien *et al.*, 2011). A study on the effect of young versus aged rodent choroid plexus secretome shows that NSC proliferation and differentiation is sensitive to age-related changes in CSF composition (Silva-Vargas *et al.*, 2016).

Direct contact with CSF also seems to affect subependymal cells *in vivo*. Upon induced ependymal damage, rodents develop subventricular glial nodules (SGNs)—defined as collections of cells, bulging into the ventricle lumen and denuded of ependyma (Gómez-Roldán *et al.*, 2008). The identity of these cells is still unclear. Some studies suggest that they are transient amplifying progenitor cells, whereas others propose neuroblasts or reactive astrocytes (Kuo *et al.*, 2006; Gómez-Roldán *et al.*, 2008; Luo *et al.*, 2008; Jiménez *et al.*, 2009; Roales-Buján *et al.*, 2012). These SGNs—also referred to as subependymal nodules or granular ependymitis—have been described in humans with multiple sclerosis or schizophrenia, and are associated with ependymal damage after viral infections and ventriculomegaly (Johnson and Johnson, 1972; Adams *et al.*, 1987; Gray *et al.*, 1992; Sarnat, 1995; Honer et al., 1996; Domínguez-Pinos *et al.*, 2005). Assumingly, SGN form when ependymal cells provide an insufficient barrier between growth factors and inflammatory mediators in the CSF and NSCs in the SVZ.

Here, we aimed to study the effect of ventricular CSF of adult humans on NSCs, by studying *post-mortem* human SVZ tissue, primary NSCs and a human immortalized NSC line. We hypothesized a stimulating effect of ventricular CSF on NSCs based on the literature, describing SGNs where CSF is in direct contact with the SVZ. Our data confirm that adult human NSCs remain in direct contact with CSF via protrusions penetrating the ependyma, but also due to significant lack of ependymal coverage. We are the first to systematically quantify SGNs in the human SVZ, to show that they are present from foetal until old age and that they express proliferation, NSC and progenitor markers, presumably due to direct CSF–NSC contact. This is supported by *in vitro* experiments, showing that human ventricular CSF induces NSC proliferation, inhibits motility and potentiates neuronal differentiation. Altogether, our results show that adult human ventricular CSF still promotes neurogenesis. This knowledge is important for initiatives exploring stimulation of endogenous NSCs as a therapeutic option for promoting brain repair in neurodegenerative diseases, but also raises the question whether CSF could play a role in the formation of brain tumours originating from mutated NSCs within the SVZ.

Materials and methods

Immunohistochemistry of human *post-mortem* tissue sections

Human brain material was obtained from the Netherlands Brain Bank (NBB). The NBB was given informed consent by brain donors for tissue use and accessing neuropathological and clinical information for scientific research, in compliance with ethical and legal guidelines (Netherlands Brain Bank, 2020).

For analysis of ependymal coverage, formalin-fixed, paraffin-embedded human *post-mortem* tissue was collected from 14 controls, classified as donors without a neurological or neuropsychiatric disorder (clinically and

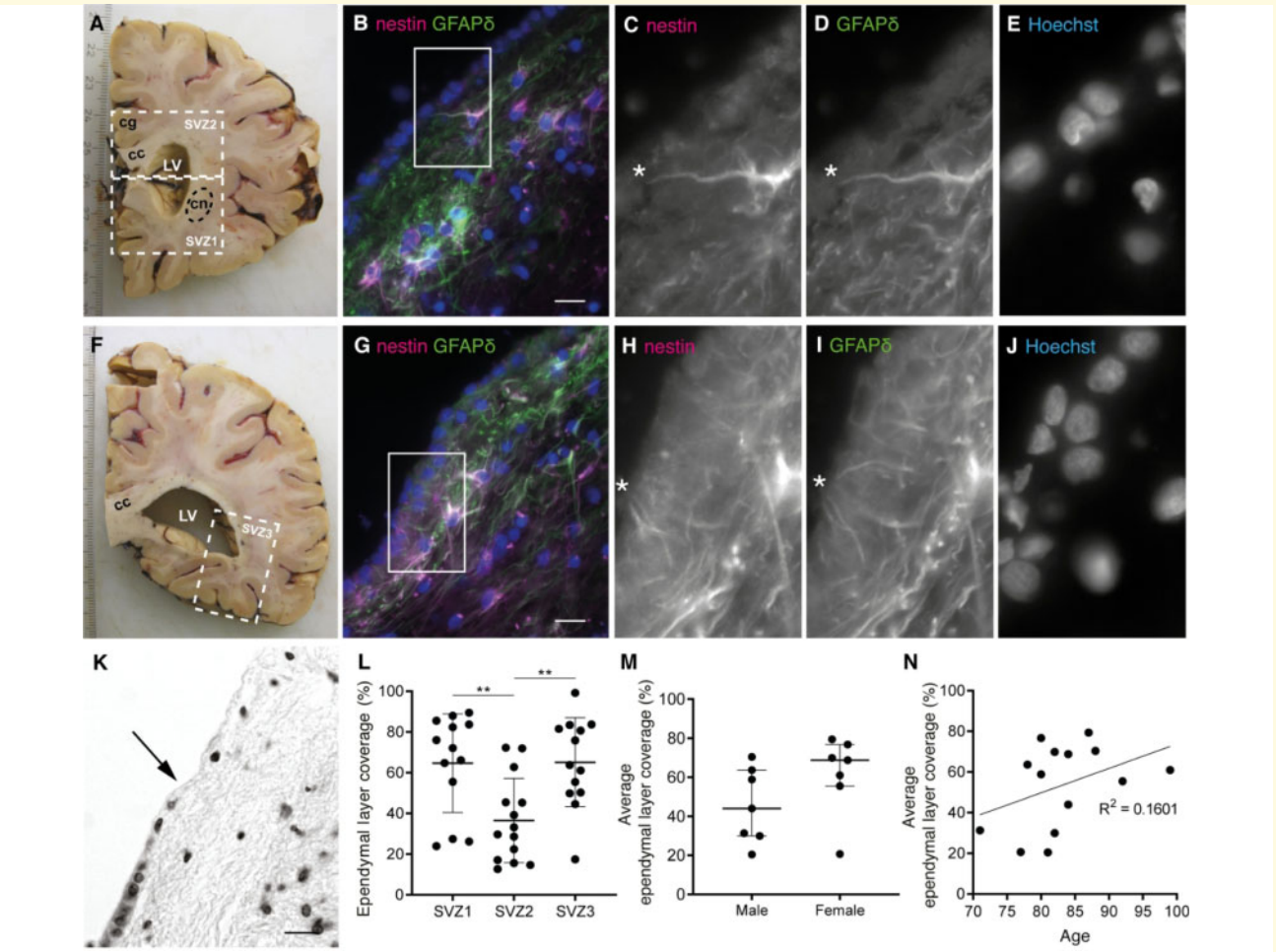

Figure 1 Contact of neural stem cells with cerebrospinal fluid through protrusions and due to the absence of ependyma covering the subventricular zone (SVZ) of adult donors. (**A, F**) White dashed lines in two 1 cm thick formalin-fixed human brain slices indicate the three dissected SVZ areas. SVZ1 was dissected in the brain slice containing the most frontal part of the caudate nucleus (cn) and SVZ2 was dissected from the same brain slice, or 1 slice more caudal, under the cingulate gyrus (cg), including part of the corpus callosum (cc). SVZ3 was dissected from the most posterior part of the lateral ventricle (LV). (**B, G**) Immunofluorescent double labelling of a fresh frozen SVZ tissue section of a control donor (NBB 2005-073, male, 87 years) for GFAPδ (green) and nestin (magenta). White rectangles and asterisks indicate protrusion(s) of NSCs towards the ventricle, of which magnifications are shown in the different channels (**C–E** and **H–J**). Nuclei are counterstained with Hoechst. (**K**) Example of thionin staining showing ependymal cell coverage and absence (transition indicated by the arrow). (**L**) Ependymal layer coverage in the SVZ of healthy controls is quantified in SVZ1-3 ($n = 13$ donors of SVZ1 and SVZ3, $n = 14$ donors of SVZ2), with significantly less ependymal cell coverage in SVZ2 (one-way ANOVA, $F(2,37) = 7.417$, $P = 0.0020$; Sidak *post-hoc* analysis, $^{**}P < 0.01$). Data are expressed as mean ± standard deviation. (**M**) Sex does not correlate with the average ependymal layer coverage over SVZ1-3 (Mann–Whitney *U* test, $U = 13$, $P = 0.1649$). Data are expressed as median ± interquartile range. (**N**) Age does not correlate with the average ependymal layer coverage in this age range (Pearson's $R^2 = 0.1601$, $P = 0.1564$). Scale bars = 10 μm.

pathologically confirmed) (Supplementary Table 1). Seven males and seven females were included, not significantly different in age ($mean_{males} = 80.6 \pm 2.0$ years, $mean_{females} = 85.9 \pm 2.9$ years; Mann–Whitney *U* test, $U = 15.50$, $P = 0.2733$). SVZ material was sampled from three lateral ventricular areas (SVZ1-3; Fig. 1A, F) and cut into 8 μm sections. One section per area per donor was deparaffinized and rehydrated. To visualize the ependymal layer, sections were incubated with 0.5% thionin (Merck) in 0.96% acetic acid for 10 min and embedded in Entellan (Merck). Thionin staining was shown to correlate significantly with staining of ependymal marker forkhead box protein J1 (FOXJ1) in quantification of the ependymal coverage (Supplementary Fig. 1).

For the analysis of SGNs, formalin-fixed paraffin-embedded human hypothalamus tissue containing part of the SVZ of the lateral and third ventricles was obtained. We analysed two to four donors per age decennium: from 2 to 94 years of age, with equal sex distribution (12 males, 14 females; two-tailed *t*-test, $t_{24} = 1.221$, $P = 0.2339$) (Supplementary Table 1). Serial sections of 6 μm were made and every 100th section were thionin-

stained. Additional single thionin-stained sections of 13 foetuses ranging in age from gestational week 9 to 40 were obtained from Bloemenhove clinic and Service Histologie-Embryologie-Cytogénétique Hôspital Necker-Enfants Malades, Paris, France. This material was from spontaneous or medically induced abortions, with maternal informed consent for use of material and access to medical records for research purposes. Tissue was collected in accordance with the Declaration of Helsinki and the Academic Medical Centre Research Code.

Immunofluorescent staining was performed as described previously (van den Berge *et al.*, 2010). Briefly, epitope retrieval was performed with citrate buffer (10 mM citric acid, 0.05% Tween-20, pH = 6.0); to block non-specific staining, sections were incubated with blocking solution (1× Tris-buffered saline [TBS, pH = 7.6], 2% horse serum, 0.1% bovine serum albumin [BSA], 0.1% TritonX-100, 0.05% Tween-20). Subsequently, sections were incubated with primary antibody (Supplementary Table 2), diluted in 1% TBS–BSA overnight at 4°C. Incubation with fluorescently labelled species-specific secondary antibodies (1:400; Jackson Immuno-Research Laboratories) was combined with Hoechst33258 (1:1000; BioRad) in TBS during 1 h. To quench autofluorescence, sections were incubated in 0.3% Sudan Black in 70% ethanol for 7 min. Sections were embedded in Mowiol (0.1 M Tris-HCl [pH = 8.5], 25% glycerol, 10% w/v Mowiol4-88 (Sigma-Aldrich)).

For 3,3′-diaminobezidine tetrahydrochloride (DAB) staining, sections were incubated with biotinylated secondary antibody (1:400; Vector Laboratories) diluted in TBS–BSA, followed by incubation with avidin–biotin complex-system (Vector Laboratories; 1:800). Subsequently, sections were incubated with DAB-solution (Sigma-Aldrich) (0.5 mg/ml in 50 mM Tris, 0.04% H_2O_2) and embedded in Entellan.

Image acquisition and quantification

All thionin-stained sections were coded for unbiased quantification. For the analysis of ependymal coverage, tiled images of the whole SVZ were taken using the AxioImagerM2 microscope (Zeiss) with a 20×/0.5 N-achroplan objective (Zeiss), AxioCamMRm camera (Zeiss) and software Zen2011 (Zeiss). Total length of SVZ bordering the lateral ventricle and length covered by ependymal cells was measured to calculate the percentage of ependymal coverage using ImageJ1.47q software (Rasband, 2015). For the analysis of SGNs, images were obtained on an AxioSkop microscope (Zeiss) with 40×/0.75 Plan-Neofluar objective (Zeiss), using an EvolutionMPColour camera (MediaCybernetics) and Image-ProPlus6.3 software (MediaCybernetics). For quantification of SGN occurrence, one thionin-stained section per foetus and between 5–10 sections per donor were scored. Fluorescently stained SVZ sections and cells were imaged using an Axioplan2 microscope (Zeiss) with 40×/0.95 Plan-Apochromat objectives (Zeiss), with Retiga2000DC camera (Qimaging) and Image-ProPlus6.3 software.

Primary human NSC isolation and culture of an immortalized human NSC line

Freshly resected SVZ material was obtained from the NBB (Supplementary Table 3). Neural stem cells from fresh SVZ tissue from three adult donors (aNSCs) were obtained based on a previously published protocol (van Strien *et al.*, 2014). Briefly, SVZ tissue was dissociated and digested with 0.2% trypsin (Invitrogen) and 0.1% DNase (Sigma-Aldrich). Subsequently, 0.2% foetal calf serum (FCS) (Gemini Bio-products) was added and cells were collected by centrifugation. Pellet was re-suspended in Dulbecco's modified Eagle's medium (DMEM) (Gibco) with 10% FCS, 1% penicillin/streptomycin (P/S) (Gibco) and 0.1% gentamycin, and filtered through a 100-µm mesh filter. Cell fraction was isolated by adding Percoll (Amersham/GE Healthcare) and centrifugation at high speed. aNSCs were isolated by CD271-coupled MicroBeads with a magnetic separation system (Miltenyi Biotec) by following the manufacturer's instruction. Foetal NSCs (fNSCs) from four donors—obtained from the AMC as described above—were isolated similarly with CD133 beads (Miltenyi Biotec). Also, a *v-myc*-mediated immortalized human NSC line (ihNSC) derived from foetal NSCs was used at low passage numbers (De Filippis *et al.*, 2007).

Human CSF

During autopsy, *post-mortem* ventricular CSF was obtained by the NBB of adult control donors (based on the clinical data) (two males, nine females; mean age, 82 years [70–94]; Supplementary Table 4). Retrospectively, two of these donors were labelled as controls with Alzheimer pathology after neuropathological examination; and two had Lewy body pathology. Cerebrospinal fluid was centrifuged at 300*g* for 5 min and pushed through a 20-µm filter to sterilize. Supernatant was stored at −80°C. Protein concentration of CSF was determined with a bicinchoninic acid assay (Pierce BCA kit; ThermoFisher Scientific). One serum sample was obtained from donor NBB 2011-082 during autopsy, and stored at −20°C.

Ante-mortem ventricular CSF was obtained during brain surgery of patients at (i) the UMC Utrecht, The Netherlands, upon approval of the Biobank Research Ethics Committee of the Central Biobank of the UMC Utrecht, and (ii) during brain surgery of patients at the Ludwig Maximilian University of Munich, Munich, Germany, after informed consent and with approval of the Ethics Committee of the Ludwig Maximilian University (four males, four females; mean age, 55 years [38–65]; Supplementary Table 4).

Lumbar CSF was obtained from 10 healthy controls (five males, five females; mean age, 65.8 years [56–79]; Supplementary Table 4) at an outpatient clinic of Amsterdam UMC, location VU University Medical Centre (VUmc), as described by Van Dijk *et al.* (2013, 2014). Donors gave informed consent for use of CSF and clinical data for research purposes, and the study protocol was approved by the VUmc ethics committee.

CSF in neurosphere cultures

After dissociation of ihNSC neurospheres, cells were plated either in ihNSC medium [Euromed-N medium (EuroClone), 1% N2 (5.375 mL DMEM-F12 (Gibco), 0.75% BSA, 62.5 mg insulin (Sigma), 100 mg apo-transferrin (Sigma), 10 µL 3 mM Na-Selenite (Sigma), 16 mg Putrescine (Sigma), 20 µg Progesterone (Sigma)), 1% glutaMAX (Gibco), 1% L-glutamin (Gibco), 1% P/S, 20 ng/mL epidermal growth factor (EGF) and 10 ng/mL fibroblast growth factor (FGF) (both from Tebu-Bio)], or in 75% ihNSC medium with 25% CSF (v/v). Similarly, aNSCs were cultured in stem-cell medium [DMEM-F12, 2% B27 (Gibco), 1% P/S, 20 ng/mL EGF, 20 ng/mL FGF], or in 75% stem-cell medium with 25% CSF (v/v). After 5 days, neurospheres were imaged (n = average of five fields per well of a 24-well plate) using a Plan-NeoFluar 10×/0.30 objective on an Axiovert200 inverted microscope (Zeiss), with EXiAqua camera (Qimaging) and Image-ProPlus6.3 software. For the ihNSCs, mean neurosphere number and diameter were determined with Image-ProPlus6.3 software. Afterwards, ihNSC neurospheres were either passaged in ihNSC medium without CSF or harvested for RNA isolation.

Single-cell motility assay of ihNSCs

Immortalized human NSCs—pre-treated with or without CSF for 5 days—were plated in DMEM-F12+glutaMAX, supplemented with 2% FCS and allowed to adhere on laminin-coated glass dishes for 6 h. Single-cell motility was analysed under a Zeiss Axiovert200 inverted microscope in a pre-heated and humidified incubation chamber (OKO Labs, Italy) at 37°C and 5% CO_2. Overnight, pictures were taken every 10 min using a Plan-NeoFluar 10×/0.30 objective with an EXiAqua camera and Image-ProPlus6.3 software. Cell motility was measured by tracking single cells throughout all frames of the sequence and measuring average velocity in µm/min using a manual tracking plugin from ImageJ (Rasband, 2015). Per condition, pictures were taken at five locations and at every location five single cells were tracked; this was repeated for three independent experiments.

RNA isolation and quantitative PCR

Cells were lysed using Trizol (Life Technologies) and RNA was isolated by organic extraction method using chloroform and ethanol precipitation and rehydration. The RNA concentrations were measured using Nanodrop1000 (ThermoFisher Scientific). Next, cDNA was synthesized from 0.5 µg RNA using the Quantitect reverse transcriptase kit (Qiagen). The relative quantity of the different cDNA fragments was determined using quantitative PCR (qPCR) as described previously (Kamphuis *et al.*, 2012; SYBR Green, Applied Biosystems). Primers used for qPCR are listed in Supplementary Table 2.

Immunofluorescent double labelling of ihNSCs

For immunocytochemistry, untreated and CSF-treated ihNSC neurospheres were dissociated and plated onto laminin-coated coverslips (3 h at 37°C, 10 µg/mL, Sigma-Aldrich) in a 24-well plate in ihNSC medium. Cells were allowed to adhere for 6 h, fixed with 4% paraformaldehyde and incubated with primary antibodies diluted in supermix (50 mM Tris, 0.15 M NaCl, 0.25% gelatin, 0.5% TritonX-100, pH = 7.4) at 4°C for 24 h. Then, cells were incubated with secondary antibodies (1:1200) and Hoechst 33258 (1:1000) in supermix at room temperature for 2 h, followed by Mowiol-embedding.

Differentiation assay of fNSCs and ihNSCs

To induce astrocytic differentiation, 2.5×10^4 cells were seeded on laminin-coated wells of a 24-well plate in DMEM-F12+glutaMAX, supplemented with 1% FCS and 1% P/S. To induce neuronal differentiation, 2.5×10^4 cells were seeded on laminin-coated wells of a 24-well plate in DMEM-F12+glutaMAX and Neurobasal medium (Invitrogen) (1:1) [0.5% N_2, 12.5 ng/mL insulin, 20 mM L-glutamin, 0.25 µM non-essential amino acids (Sigma-Aldrich, St. Louis, USA), 1% B27 and 1% P/S].

Statistical analysis

GraphPad Prism7.04 (GraphPad Software) and SPSS version 23 (IBM) were used to analyse data for statistical significance. No sample size calculations were done; the pre-set n per experiment—as described in the legend of each figure—was determined mainly by the limited amount of human material available. The F test, respectively, Bartlett's test was applied to test for equality in variances; the D'Agostina and Pearson test was used to test normality. For normally distributed data sets with equal variances, the two-tailed or paired t-test, or one-way *ANOVA* with Sidak *post-hoc* analysis was used. For data sets with unequal variances, the two-tailed t-test with Welch's correction was used. For data sets violating the assumption of normality, the Mann–Whitney U test, Wilcoxon matched-pairs test or Kruskal–Wallis test with Dunn's *post-hoc* analyses was used. To test correlation, Pearson's correlation, Fisher's exact test or logistic

regression was used. Statistical significance was accepted when $P < 0.05$. Data are expressed as mean ± standard deviation, or median ± interquartile range; when fold change is presented, the data are normalized against the control group (no CSF).

Data availability

Raw data were generated at the Netherlands Institute for Neuroscience (Amsterdam, The Netherlands) and the UMC Utrecht Brain Centre (University Medical Centre Utrecht, Utrecht, The Netherlands). Derived data supporting the findings of this study are available from the corresponding author on request.

Results

Neural stem cells in adult SVZ are exposed to CSF via protrusions through ependyma or due to lack of ependyma

The ependymal cell layer forms the CSF–brain barrier. To determine whether NSCs in the human SVZ of adult donors are in direct contact with CSF, fresh frozen adult human SVZ sections were double-labelled for NSC markers glial fibrillary acidic protein delta (GFAPδ) and nestin. Ependymal cells were clearly visible based on nuclear staining. We observed many GFAP$^+$δ/nestin$^+$ cells lining the ventricle and several double-positive cells had protrusions through the intact ependyma towards the ventricle (Fig. 1B–E, G–J), suggesting that NSCs in the SVZ of adult humans remain in close contact with CSF.

We also studied whether the CSF–brain barrier was intact by visualizing the ependymal layer with thionin staining in three different SVZ regions (Fig. 1A and F) in adult control donors and assessing the coverage percentage of the SVZ (Fig. 1K). There was profound absence of ependymal cells in all donors, with an average lack of around 50% and significantly less ependymal coverage in SVZ2 compared to SVZ1 and 3 (Fig. 1L). Ependymal coverage did not correlate with sex or age (Fig. 1M and N) nor with donor's *post-mortem* delay (Pearson $R^2 = 0.0090$, $P = 0.7473$), fixation time (Pearson $R^2 = 0.001236$, $P = 0.9050$), CSF pH (Pearson $R^2 = 0.0642$, $P = 0.4034$) or brain weight (Pearson $R^2 = 0.0216$, $P = 0.6165$).

Subventricular nodules are present from birth until old age, and express NSC and progenitor markers

Subventricular glial nodules are defined as hypercellular nodules bulging into the ventricular space, denuded of ependyma. The incidence of SGNs in the healthy human brain has not been assessed before. Therefore, its presence was scored on thionin-stained human hypothalamic sections of control donors ranging from 2 to 94 years (Supplementary Table 1). Often, SGNs contained dense fibrous material, which might represent either cellular extensions or acid mucopolysaccharides in the extracellular matrix (Fig. 2A and B). The SGNs ranged in diameter from 100 to 500 µm and were observed in 69.2% (18/26) of the donors, mostly in the wall of the lateral ventricle (Supplementary Table 1). The occurrence of SGN was not related to sex (Fisher's exact test, $P = 0.4009$). Also, no significant correlation was found with age although a positive trend was noted (Fig. 2C). Donor's *post-mortem* delay (Mann–Whitney U test, $U = 40$, $P = 0.2316$) and brain weight (Mann–Whitney U test, $U = 38$, $P = 0.1869$) were unrelated to SGN incidence, fixation time was related to SGN score (Mann–Whitney U test, $U = 35.50$, $P = 0.0420$) with lower fixation times for the donors scored to have SGNs. Among the 13 foetal sections, only one brain showed two SGNs.

The cellular composition of SGNs was unravelled with immunofluorescence. The SGNs stained positive for NSC markers nestin, GFAPδ (Fig. 2D) and sex-determining region box 2 (SOX2, Fig. 2E), proliferation marker proliferating cell nuclear antigen (PCNA, Fig. 2F) and transit-amplifying progenitor marker epidermal growth factor receptor (EGFR, Supplementary Fig. 2A). The SGNs were also immunopositive for vimentin (Fig. 2E)—a marker for immature and reactive astrocytes—and S100β (Supplementary Fig. 2B)—a mature astrocyte marker—but were devoid of immature and mature neuronal marker βIII-tubulin, oligodendrocyte precursor marker βIV-tubulin and microglia marker HLA-DR (Supplementary Fig. 2C–E). As GFAPα is not highly expressed in SGNs (Fig. 2G), reactive gliosis seems unlikely. Overall, this indicates a local accumulation of proliferating NSCs and progenitor cells without apparent gliosis.

Adult ventricular CSF increases and lumbar CSF decreases NSC proliferation *in vitro*

Our *in vivo* data may indicate that exposure to ventricular CSF leads to accumulations of NSC and progenitor cells in SVZ denuded of ependyma. Therefore, we next assessed the effect of CSF on NSC proliferation *in vitro*. First, aNSCs were cultured with 25% pooled *post-mortem* ventricular CSF for 5 days and compared to non-treated aNSCs in a neurosphere assay ($n = 3$). It was observed that CSF-treated aNSCs formed larger and more neurospheres compared to untreated aNSCs (Fig. 3A). As aNSC isolation yield of brain donors is very low, remaining experiments were performed with ihNSCs. Similarly, neurospheres formed by CSF-treated ihNSCs were on average twice as large as untreated neurospheres (Fig. 3B and C).

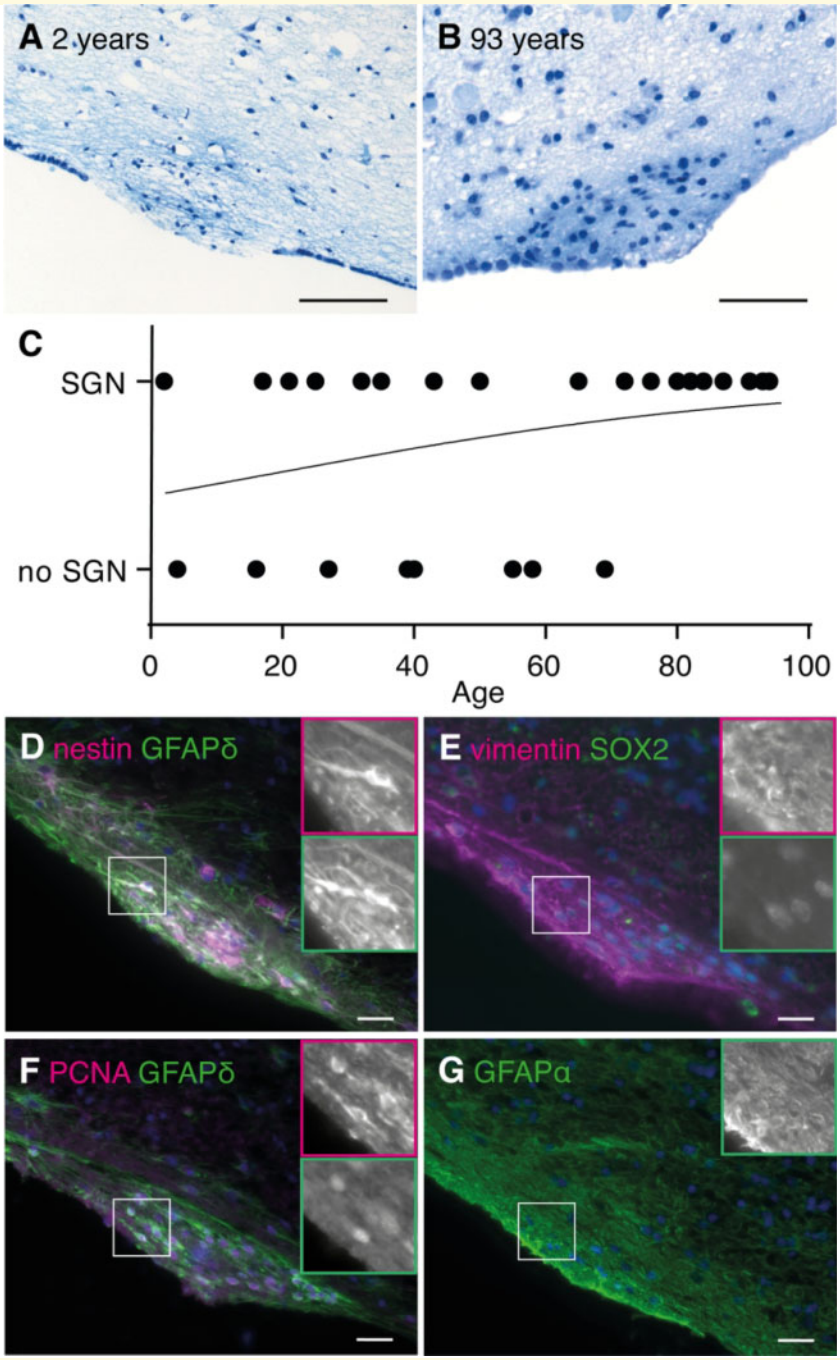

Figure 2 Subventricular glial nodules are commonly present in the human subventricular zone and express proliferation and stem cell markers. (**A, B**) SGN in the lateral ventricle of a 2-year-old male donor (NBB 1997-017, scale bar 100 μm) and a 93-year-old female donor (NBB 2005-063, scale bar 50 μm), being denuded of ependyma, hypercellular and showing accumulation of thionin-positive fibrous tissue. (**C**) No significant correlation was found between age and SGN occurrence (Cox–Snell's $R^2 = 0.1004$, $\chi^2(1) = 2.750$, $P = 0.0972$). (**D–F**) SGNs express NSC (nestin, GFAPδ and SOX2), astrocyte (vimentin) and proliferation (PCNA) markers. (**G**) GFAPα is not specifically expressed by SGNs (NBB 2005-073, male, 87 years). Scale bars C–F = 10 μm.

Also, the number of neurospheres was significantly increased (Fig. 3B and D). This indicates that human ventricular CSF contains neurogenic factors. Although *post-mortem* delay was short (<7 h) in our CSF donors, it was tested whether *ante-mortem* ventricular CSF had a similar effect on ihNSCs. In accordance with the *post-mortem* CSF finding, ihNSCs exposed to *ante-mortem* ventricular CSF formed larger neurospheres as compared to untreated ihNSCs (Supplementary Fig. 3A). To investigate whether the effect of ventricular CSF treatment is long lasting and

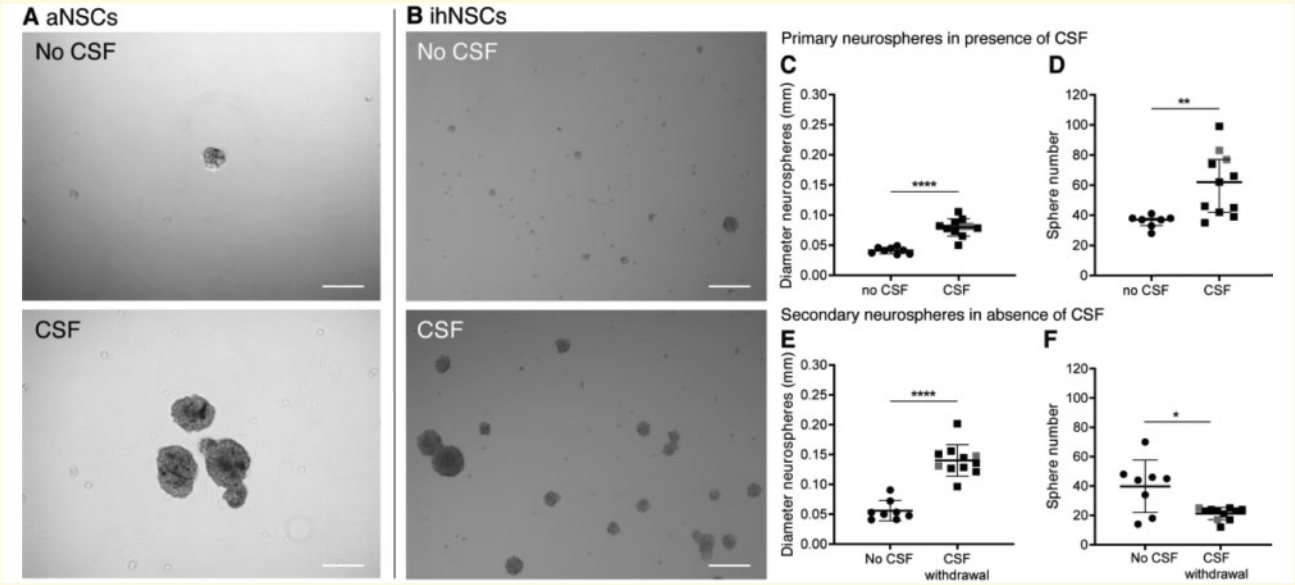

Figure 3 Increased neural stem cell (NSC) proliferation upon treatment with ventricular CSF. (**A**) Representative image of primary adult NSC (aNSC) culture of donor NBB 2012-066. aNSCs treated with 25% pooled *post-mortem* ventricular CSF were observed to form more and larger neurospheres than untreated aNSCs after 5 days in culture. (**B**) Representative image of immortalized human NSC (ihNSC) culture without and with CSF of donor NBB 2011-096. ihNSCs treated with 25% *post-mortem* ventricular CSF ($n = 11$ wells treated with CSF of individual donors) form larger and more neurospheres compared to untreated cells ($n = 8$ untreated wells) after 5 days. (**C, D**) The ihNSC neurosphere diameter (two-tailed *t*-test with Welch's correction, $t_{13.39} = 8.13$, $P < 0.0001$) and sphere number (Mann–Whitney *U* test, $U = 6$, $P = 0.0018$) were quantified after 5 days of CSF treatment. (**E, F**) Seven days after CSF withdrawal, passaged ihNSC neurosphere diameter (two-tailed *t*-test, $t_{17} = 7.877$, $P < 0.0001$) and number (two-tailed *t*-test with Welch's correction, $t_{7.558} = 2.887$, $P = 0.0216$) were quantified. In grey, the data points belonging to the wells treated with CSF of Alzheimer patients are indicated; exclusion of these data points did not change the statistical results. Data expressed as mean ± standard deviation in C, E and F, and as median ± interquartile range in D; $^{*}P < 0.05$, $^{**}P < 0.01$, $^{****}P < 0.0001$; Scale bars = 100 μm.

remains after CSF withdrawal, CSF-treated ihNSC neurospheres were dissociated, washed and plated in ihNSC medium containing EGF and FGF without CSF. After 7 days, neurosphere size in the CSF-withdrawn condition was still significantly larger compared to ihNSCs not exposed to CSF (Fig. 3E). In contrast, secondary neurosphere number was decreased (Fig. 3F).

To exclude the possibility that contamination of ventricular CSF with blood-derived factors—which might have occurred during puncturing of the lateral ventricle—could be responsible for the increased proliferation of ihNSCs, 50% of *post-mortem* CSF, respectively, different concentrations of serum of the same donor was added to a neurosphere assay. After 5 days, the number of neurospheres formed was lower when ihNSCs were treated with serum compared to CSF (Supplementary Fig. 3B). Also, protein concentration in CSF was lower than the lowest concentration of serum used in the neurosphere assay, implying that if there is contamination it can only be a minute fraction.

The effect of lumbar CSF was also assessed, and it was observed that adding 25% of lumbar CSF led to the formation of smaller and a decreased number of neurospheres after 5 days in culture. In addition, the lumbar CSF-treated ihNSCs adhered more to the cell-culture plate, compared to untreated ihNSCs (Fig. 4A–C). Altogether these data show that ventricular CSF, but not lumber CSF, has a specific composition which stimulates NSC growth and survival.

Adult ventricular CSF decreases NSC motility *in vitro*

Progenitors derived from SVZ NSCs normally migrate towards the rostral migratory stream. Since SGNs are local accumulations of NSCs, it was tested whether contact with *post-mortem* ventricular CSF affects NSC motility *in vitro*. Average velocity of untreated and CSF-pretreated ihNSCs was measured overnight by tracking cell movement with time-lapse imaging. Cerebrospinal fluid-pretreated ihNSCs showed a significant decrease in average velocity compared to untreated ihNSCs (Fig. 5A). Furthermore, the morphology of CSF-pretreated ihNSCs was changed, as CSF-pretreated cells were more extended and showed more protrusions compared to untreated ihNSCs (Fig. 5B), suggesting an enhanced interaction with the cell-culture surface potentially causing decreased ability to migrate upon CSF exposure.

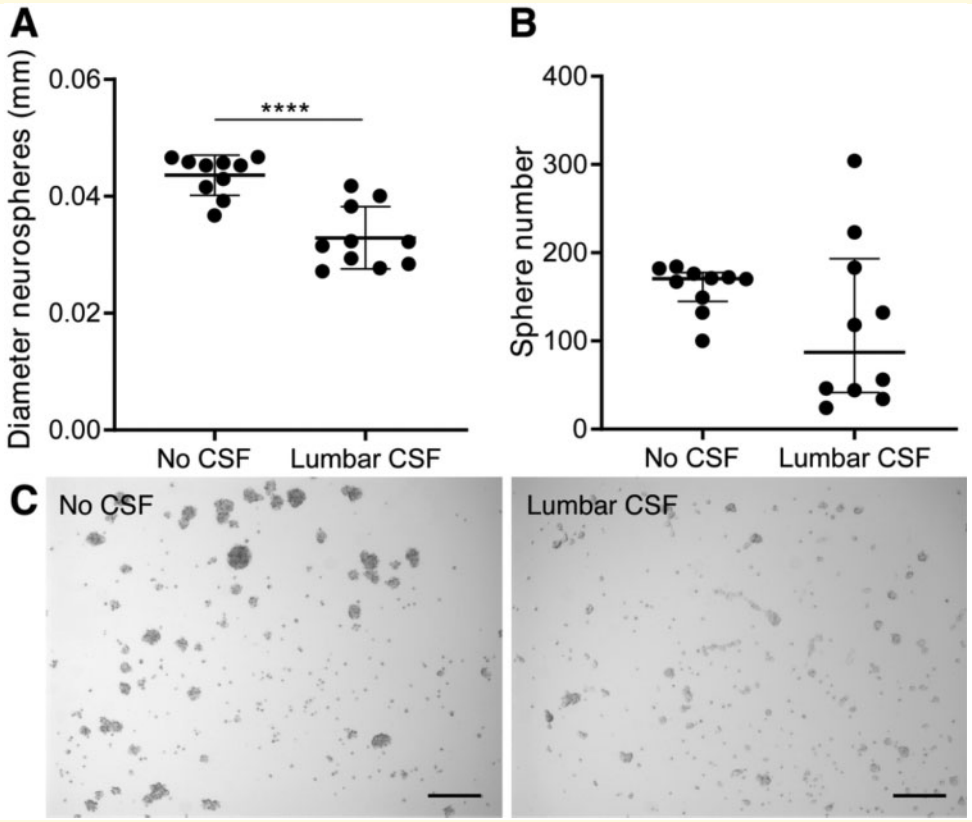

Figure 4 Decreased NSC proliferation upon treatment with lumbar CSF. (**A**) Immortalized human NSCs (ihNSCs) treated with 25% lumbar CSF ($n = 10$ wells treated with CSF of individual healthy controls) form smaller neurospheres compared to untreated cells ($n = 10$ untreated wells) after 5 days (two-tailed *t*-test, $t_{18} = 5.364$, $P < 0.0001$). Data are expressed as mean ± standard deviation; ****$P < 0.0001$. (**B**) ihNSCs tend to form less neurospheres when exposed to lumbar CSF (Mann–Whitney *U* test, $U = 31.50$, $P = 0.1717$). Data are expressed as median ± interquartile range. (**C**) After 5 days of treatment with lumbar CSF, ihNSCs adhere more to the bottom of the well and form smaller and less neurospheres compared to untreated ihNSCs. Representative image of neurosphere culture of with CSF of donor G022. Scale bars = 100 μm.

Adult ventricular CSF initiates NSC activation

Next, the effect of *post-mortem* ventricular CSF on NSC activation was assessed by testing indicators of the Notch signalling pathway. It was observed that 5-day CSF treatment of ihNSCs led to higher mRNA expression of Notch homolog 1 (*NOTCH1*), hes family bHLH transcription factor 5 (*HES5*), Jagged1 (*JAG1*) and presenilin 1 (*PSEN1*) and a positive trend in the expression of hes family bHLH transcription factor 1 (*HES1*) (Supplementary Fig. 4).

Subsequently, the effect of CSF on NSCs was determined by measuring mRNA expression changes of several NSC, progenitor and mature neuronal and astrocytic markers (Fig. 6A, Supplementary Table 5). Nestin (*NES*), NSC/astrocyte marker *GFAP*α and *GFAP*δ were significantly highly expressed in ihNSCs exposed to CSF (Fig. 6B and C). For comparison, fNSCs were allowed to differentiate, and showed an increase of *GFAP*α and *GFAP*δ expression and a decrease in *GFAP*δ/α ratio at day 1 of differentiation (Supplementary Fig. 5A–C). Accordingly, upon CSF exposure, *GFAP*δ/α—high in NSCs and lower in astrocytes (Roelofs *et al.*, 2005; Middeldorp *et al.*, 2010)—is also lower in ihNSCs, which suggests that NSCs are activated and started to differentiate. Correspondingly, mRNA expression of nerve growth factor receptor (*NGFR*)—expressed by NSCs in the adult human brain—showed negative trend upon CSF treatment. Accordingly, the expression of late precursor and mature astrocyte marker glutamine synthetase (*GLUL*) and mature astrocyte progenitor marker solute carrier family 1 member 2 (*SLC1A2*) was increased after CSF treatment. Mature astrocyte markers fibroblast growth factor receptor 3 (*FGFR3*) and *S100*β were not significantly altered. Furthermore, neural progenitor and proneural marker achaete–scute family bHLH transcription factor 1 (*ASCL1*), neuroblast marker doublecortin (*DCX*), immature neuronal marker neural cell adhesion molecule 1 (*NCAM1*) and immature and mature neuronal marker βIII-tubulin (*TUBB3*) were significantly higher expressed after CSF treatment. Altogether, these data show that upon CSF treatment NSCs transit to a more

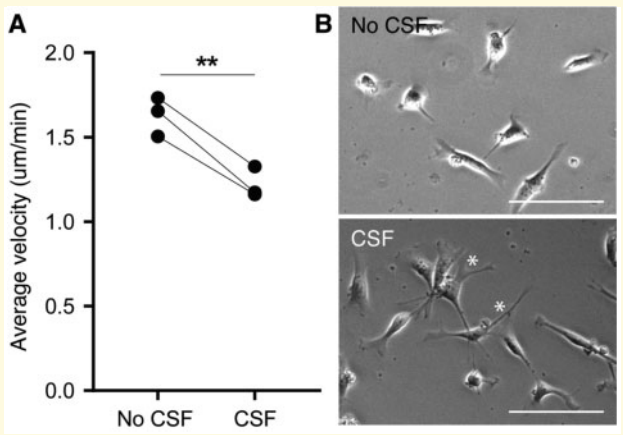

Figure 5 Decreased cell motility and changed morphology of ihNSCs after ventricular CSF pre-treatment. (**A**) Average velocity of cells pre-treated with CSF ($n = 3$ culture replicates) was significantly lower compared to untreated cells ($n = 3$ culture replicates) (paired *t*-test, $t_2 = 10.17$, $P < 0.0095$). Per-culture replicate, five cells were traced per five locations per condition. Data are expressed as mean ± standard deviation. (**B**) Representative phase-contrast pictures of untreated ihNSCs and ihNSCs pre-treated with CSF; the former showing rounder cells, the latter showing a more elongated morphology with more protrusions (*). Scale bars = 100 μm.

active state with up-regulation of Notch, astrocyte and neuronal progenitor markers.

Cerebrospinal fluid-induced transition of NSCs to progenitors was confirmed by immunofluorescence staining for the presence of nestin and SOX2, and pan-GFAP and βIII-tubulin protein. In untreated ihNSCs, the levels of GFAP and βIII-tubulin protein were below detection (Fig. 6E). After treatment with pooled CSF for 5 days (Fig. 6D and E), ihNSCs were still immunopositive for nestin and SOX2, but also showed a clear increase in pan-GFAP and βIII-tubulin immunofluorescence. These results corroborate the changes in RNA expression after CSF treatment. Altogether, the data show that upon CSF exposure, NSCs become more activated and primed towards proliferating progenitor cells since they not only express NSC markers, but also show increased expression of Notch, astrocyte and neuronal progenitor markers.

Adult ventricular CSF suppresses differentiation of NSCs into astrocytes

In the following experiment, differentiation of ihNSCs was assessed by culturing cells after 5 days of CSF exposure, in astrocyte or neuronal differentiation medium without CSF. Pre-treated ihNSCs cultured for 2 days in astrocyte differentiation medium showed unchanged mRNA levels of *NES* and *NGFR* and a positive trend in *GFAP*α and *GFAP*δ expression (Supplementary Fig. 6A), mimicking the expression pattern seen in differentiating fNSCs as discussed earlier. The *GFAP*δ/α ratio was not significantly altered compared to untreated ihNSCs. Additionally, expression of astrocyte markers *FGFR3*, *SLC1A2* and *S100*β and neuronal markers *TUBB3* and *NCAM1* did not change, whereas neuronal precursor markers *ASCL1* and *DCX* showed a positive trend. It suggests that CSF pre-exposure primes NSCs to differentiate into the astrocytic as well as neuronal lineage, even within an astrocytic differentiation protocol. This is supported by immunohistochemical stainings after 7 days of astrocytic differentiation that shows similar expression of GLUL and S100β, and increased immunoreactivity of FGFR3, GFAPδ and DCX, compared to ihNSCs not pre-treated with CSF (Supplementary Fig. 6B–D).

Yet, a longer differentiation time showed a repression of astrocyte differentiation after CSF pre-exposure. In ihNSCs that were allowed to differentiate after a 7-day astrocytic differentiation protocol, all NSC and astrocytic (progenitor) markers showed a clear negative trend, yet not significant (Fig. 7A). The 7-day neuronal differentiation protocol resulted in an unchanged mRNA expression of NSC and neuronal (progenitor) markers (Fig. 7B). These results indicate that CSF pre-exposure primes NSCs to differentiate into neuronal over astrocytic lineage.

Discussion

In this study, we used human *in vitro* models to show that adult human ventricular CSF induces NSC proliferation, inhibits NSC motility and potentiates neuronal differentiation. We also demonstrate that NSCs in the SVZ of adult humans remain in contact with CSF via protrusions through an intact ependymal layer and even more so due to extensive lack of ependymal coverage. We reveal accumulation of proliferating neural stem and progenitor cells at places where the neurogenic niche is denuded of ependyma, and are the first to quantify systematically the presence of these so-called SGNs in the human SVZ and show that they are present from foetal until old age. This indicates that CSF is an important regulator of neurogenesis in humans throughout life.

An intact ependymal layer forms a semi-permeable barrier, allowing a controlled exchange of factors between CSF and brain parenchyma. Ependymocytes are post-mitotic cells that arise from radial glia during embryonic development. It has been shown that these cells do not have the capacity to regenerate (Spassky, 2005). In mice, however, an increasing number of astrocytes—sharing characteristics of ependymocytes—is interposed within the ependymal layer with aging (Luo *et al.*, 2006, 2008). This form of ependymal repair is associated only with mild denudation adjacent to an active neurogenic niche (Luo *et al.*, 2008), suggesting that an active neurogenic niche needs an intact CSF–brain barrier for normal functioning. Also, it suggests that an active SVZ and/or

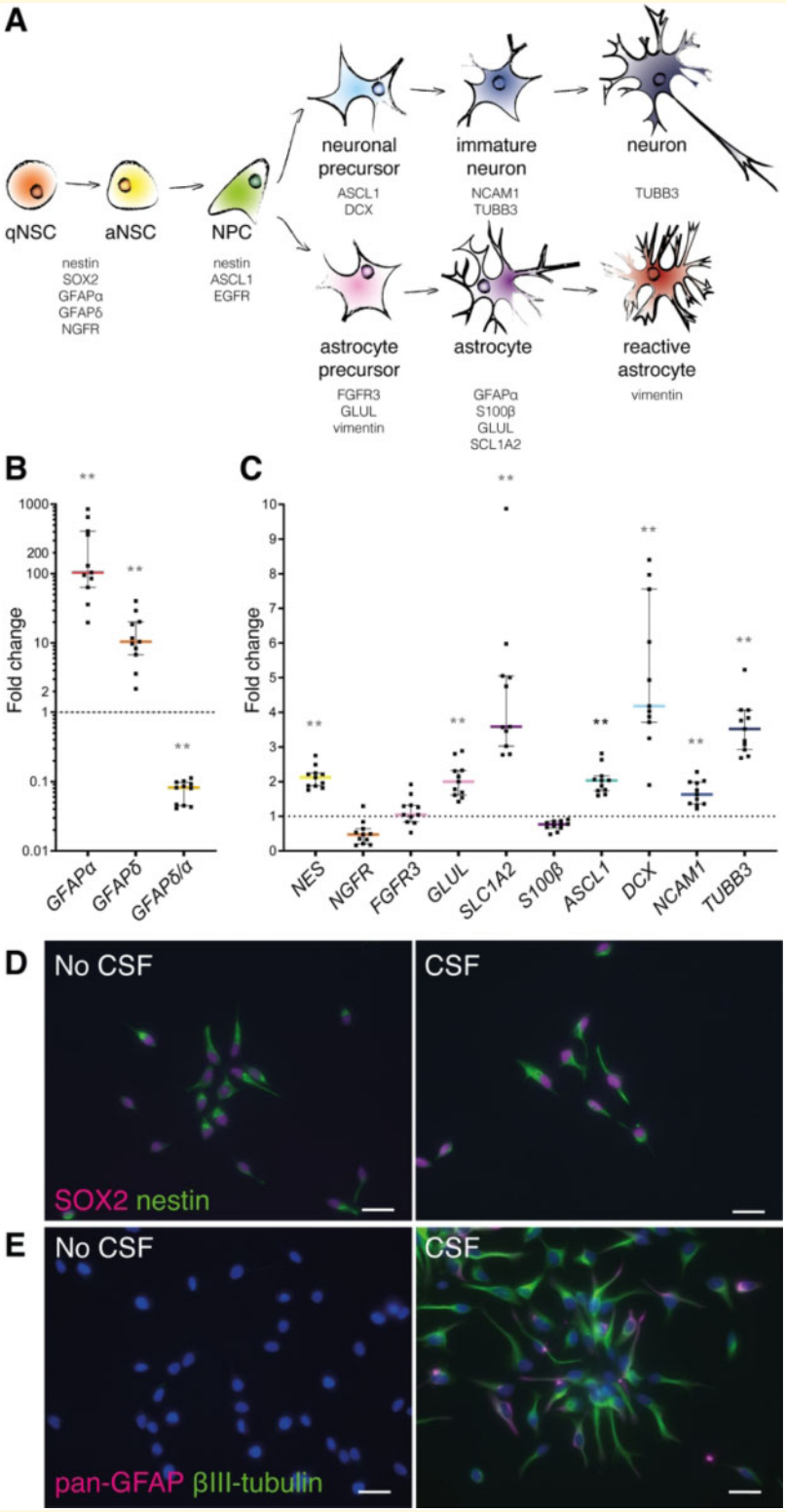

Figure 6 Upon treatment with ventricular CSF, ihNSCs transition to a more active state with up-regulation of astrocyte and neuronal progenitor markers. (**A**) Schematic overview of markers used to characterize the effect of CSF on lineage progression (for references, see Supplementary material Table 5). qNSC = quiescent NSC; aNSC = activated NSC; NPC = neural progenitor cell. (**B,C**) After 5 days of CSF treatment, cells were collected and used for mRNA expression analysis ($n = 6$ untreated wells, $n = 11$ wells treated with CSF of individual donors); AluS, elongation factor 1-alpha (EF1α) and actin were used as reference genes. *GFAPα* (Mann–Whitney *U* test, $U = 0$, $P = 0.00016$), *GFAPδ* (Mann–Whitney *U* test, $U = 0$, $P = 0.00046$) and *NES* (Mann–Whitney *U* test, $U = 0$, $P = 0.00016$) were higher, whereas the ratio *GFAPδ/α* (Mann–Whitney *U* test, $U = 0$, $P = 0.00046$) was lower expressed compared to untreated ihNSCs. *NGFR* (Mann–Whitney *U* test, $U = 11$, $P = 0.0273$), *FGFR3* (Mann–Whitney *U* test, $U = 23$, $P = 0.350$) and *S100β* (Mann–Whitney *U* test, $U = 0$, $P = 0.00016$) were not

(continued)

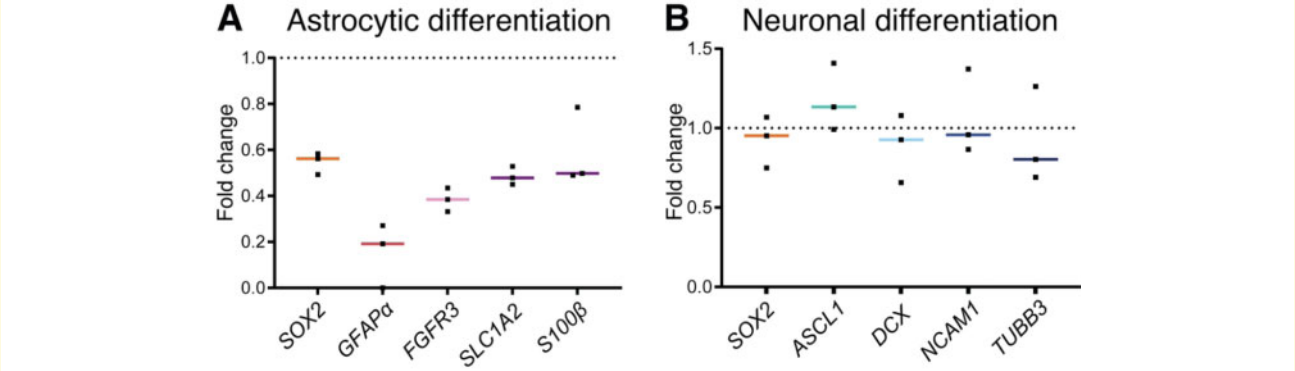

Figure 7 Ventricular CSF exposure (7 days) primes ihNSCs to differentiate into neuronal over astrocytic lineage upon CSF withdrawal. (**A**) CSF-treated ihNSCs were differentiated according to astrocytic differentiation protocol upon CSF withdrawal (culture replicates, $n = 3$). Per-culture replicate, ihNSCs were untreated, respectively, pre-treated with pooled CSF of healthy controls. After 7 days, mRNA levels of *SOX2* (Mann–Whitney *U* test, $U = 0$, $P = 0.1000$), *GFAPα* (Mann–Whitney *U* test, $U = 0$, $P = 0.2000$), *FGFR3* (Mann–Whitney *U* test, $U = 0$, $P = 0.1000$), *SLC1A2* (Mann–Whitney *U* test, $U = 0$, $P = 0.1000$), *S100β* (Mann–Whitney *U* test, $U = 1$, $P = 0.2000$) were measured. (**B**) Seven days later, ihNSCs were allowed to differentiate according to neuronal differentiation protocol (culture replicates, $n = 3$), after pre-treatment with pooled CSF, mRNA levels of *SOX2* (Mann–Whitney *U* test, $U = 3$, $P = 0.7000$), *ASCL1* (Mann–Whitney *U* test, $U = 1$, $P = 0.2000$), *DCX* (Mann–Whitney *U* test, $U = 3$, $P = 0.7000$), *NCAM1* (Mann–Whitney *U* test, $U = 4$, $P > 0.9999$) and *TUBB3* (Mann–Whitney *U* test, $U = 4$, $P > 0.9999$) were measured. Per-culture replicate, ihNSCs were untreated, respectively, pre-treated with pooled CSF of healthy controls. Actin, AluS and glyceraldehyde-3-phosphate dehydrogenase (GAPDH) were used as reference genes. Data are expressed as median fold change of relative mRNA expression of pre-treated ihNSCs over relative expression of untreated ihNSCs (dotted line); *Sidak* corrected *P* value = 0.0102.

contact with existing ependymocytes is necessary to generate intercalating astrocytes. When greater loss of contiguous ependymal cells is induced in rodents, astrocytes are unable to take on characteristics of ependymal cells and SGNs are formed instead (Kuo *et al.*, 2006; Gómez-Roldán *et al.*, 2008; Luo *et al.*, 2008; Jiménez *et al.*, 2009; Roales-Buján *et al.*, 2012; Muthusamy *et al.*, 2015). As SGNs do not specifically express GFAPα or HLA-DR, a local immune reaction or reactive gliosis seems unlikely. Instead, our data indicate that SGNs are composed of accumulated proliferating neural stem and progenitor cells, and hence corroborating our *in vitro* findings that CSF stimulates proliferation and differentiation of NSCs and inhibits motility.

The effect we describe about human CSF on NSC proliferation is in agreement with the results of Zhu *et al.* (2015), showing that human *ventricular* CSF from hydrocephalic patients promotes proliferation of human foetal neural progenitor cells (NPCs), and the data of Buddensiek *et al.* (2010) indicating that human *lumbar* CSF from hydrocephalic patients reduces adult human NSC proliferation *in vitro*. We ascribe these seemingly opposite findings to differences in origin, and therefore composition, of the CSF as gradual changes in CSF composition along the flow pathway between the brain and lumbar sac have been described, forming a rostral–caudal gradient of factors (Sommer *et al.*, 2002; Brandner *et al.*, 2014). In agreement with the proliferation/migration dichotomy stating that proliferation and migration temporally are mutually exclusive behaviours (Giese *et al.*, 1996), we observed a decreased motility of NSCs after pre-treatment with CSF *in vitro*. These results seem in contrast with the findings of Zhu *et al.* (2015)—who found an increase in speed, travel distance and migration capacity of NPCs upon CSF treatment—possibly due to differences in their experimental set-up—i.e. measuring motility on polyurethane acrylate–nanopatterns with poly-L-ornithine and laminin-coating after CSF pre-treatment

differentially expressed, whereas *GLUL* (Mann–Whitney *U* test, $U = 0$, $P = 0.00016$) and *SLC1A2* (Mann–Whitney *U* test, $U = 0$, $P = 0.00016$) were higher expressed. *ASCL1* (Mann–Whitney *U* test, $U = 0$, $P = 0.00016$), *DCX* (Mann–Whitney *U* test, $U = 2$, $P = 0.000646$) and *NCAM1* (Mann–Whitney *U* test, $U = 2$, $P = 0.000646$) as well as *TUBB3* (Mann–Whitney *U* test, $U = 0$, $P = 0.00016$) were highly expressed compared to untreated ihNSCs. Exclusion of data points belonging to the assays treated with CSF of Alzheimer patients did not change the statistical results. Data are expressed as median fold change of relative mRNA expression of CSF-treated ihNSCs over relative expression of untreated ihNSCs (dotted line) ± interquartile range; *Sidak* corrected *P* value = 0.0039 for multiple comparisons, $^{*}P < 0.0039$, $^{**}P < 0.001$, $^{***}P < 0.0001$, $^{****}P < 0.00001$. (**D**) ihNSCs were treated with 25% pooled CSF in ihNSC medium for 5 days and labelled for SOX2 (magenta) and nestin (green). (**E**) CSF-treated ihNSCs were also stained for the astrocyte marker pan-GFAP (magenta) together with βIII-tubulin (green). Hoechst (blue) as nuclear counter staining. Scale bars = 10 μm.

of undescribed duration, and measuring migration using a transwell assay with glioma-conditioned medium as attractant for NPCs treated with CSF during 7 and 14 days, all in differently composed media.

Based on the neurosphere assays and RNA analyses—and in agreement with the observed formation of SGNs where ependyma is lacking—we conclude that ventricular CSF pushes NSCs from a relative quiescent into a more active state, being more proliferative and capable of self-renewal as well as being less motile. Second, when CSF is withdrawn, NSCs develop into a progenitor state, still highly proliferative but less capable of self-renewal—i.e. larger neurosphere size but lower neurosphere number. The idea that NSCs exposed to CSF become more activated is supported by our mRNA expression and immunohistochemical data showing a general increase in RNA and protein levels in NSCs after CSF treatment. Indeed, NSC activation is characterized by up-regulation of protein synthesis, and subsequent cell division (Baser *et al.*, 2017). Also, *ASCL1* expression increases upon CSF exposure, which has been shown to promote NSC activation and proliferation (Andersen *et al.*, 2014). Furthermore, self-renewal and maintenance of activated NSCs is believed to be regulated by Notch1, whereas quiescent NSCs seem less reliant on Notch1 signalling (Basak *et al.*, 2012; Engler *et al.*, 2018); we see clear *NOTCH1* up-regulation and activation of the Notch pathway after CSF treatment. Thus, our data indicate that CSF of adult humans activates NSCs, and hence promoting proliferation and priming NSCs to differentiate. Additionally, we found an indication that CSF promotes neuronal over astrocytic differentiation. Interestingly, Schwarz *et al.* (2017) have shown that human lumbar CSF improves survival and enhances network function of neurons *in vitro*. Also, Veening and Barendregt (2010) describe that *in vivo* neurons in the SVZ are in contact with CSF via processes that terminate in the ventricle and actively release neuromodulators in the CSF that can exert downstream effects on target neurons. These observations hint that CSF might not only potentiate neuronal differentiation, but also impact mature neurons.

The use of *post-mortem* material is a strength as well as a weakness of our study. We were able to use brain tissue slides of a total of 40 adult human donors and 13 human foetuses, and *post-mortem* CSF of 10 human donors—these are large numbers with respect to most of the previous literature. Limitations are related to the characterization of the *post-mortem* donors. Working with *post-mortem* material entails that when used directly after autopsy, only clinical information is available, based on which donors are included as controls. Later pathological assessment changed donor status of two CSF donors into controls having early stages Alzheimer pathology (Braak 3-4)—importantly, their clinical files underscore that there was no clinical phenotype yet. As there was no difference found between CSF of these particular donors and other donors in experiments in which CSF of single donors was used, the experiments with pooled CSF—composed of CSF of controls and two donors with Alzheimer pathology—were included in this article. Similarly, the donors of aNSCs were eventually classified as donors with Alzheimer's disease, Korsakov's syndrome and bipolar disorder. As the effect of CSF on aNSCs of the different donors was similar and also showed the same pattern observed in ihNSCs, the aNSCs of these donors were regarded as useful models. Second, as *post-mortem* ventricular CSF is more readily available, obtainable in larger volumes and giving the same results in experiments as *ante-mortem* ventricular CSF, mainly *post-mortem* CSF was used in this study. Since the composition of CSF may change after death, only CSF samples with a short *post-mortem* delay (<7 h) were included.

The potential of CSF to stimulate neurogenesis is clinically relevant in two ways. The most common neurodegenerative diseases in elderly—Alzheimer's and Parkinson's disease—are characterized by extensive neuronal degeneration. Our previous studies have shown that NSCs are still present in the SVZ of these patients, and are still able to proliferate and differentiate into neurons and glial cells *in vitro* (van den Berge *et al.*, 2011; van Strien *et al.*, 2014). Stimulation of endogenous NSCs in SVZ of patients with a neurodegenerative disorder could therefore potentially lead to neuronal replacement. The fact that we show that CSF promotes neuronal over astrocytic lineage differentiation is interesting in this respect. Second, it has been hypothesized that mutated NSCs are the initiating cells in glioma, i.e. the most common primary malignant brain tumour (Quiñones-Hinojosa and Chaichana, 2007; Jackson and Alvarez-Buylla, 2008). These glioma stem cells functionally resemble NSCs (Ignatova *et al.*, 2002; Galli *et al.*, 2004; Singh *et al.*, 2004; Jackson *et al.*, 2006), and gliomas primarily seem to arise in the SVZ (Lantos and Pilkington, 1979; Zhu *et al.*, 2005; Lim *et al.*, 2007; Chaichana *et al.*, 2008; Lee *et al.*, 2018). There are indications that gliomas arising in closer proximity to the SVZ are more likely to be of a proneural or neural subtype (Steed *et al.*, 2016); noteworthy in the light of our finding that CSF promotes neuronal lineage differentiation. Thus, understanding how CSF stimulates NSCs will also help to elucidate the contribution of CSF to gliomagenesis.

Conclusion

In conclusion, we show that ventricular CSF continues to influence NSC proliferation, motility and differentiation in adult humans, despite age-related changes in CSF composition that have been described by others. Factors in the CSF and related mechanisms responsible for these effects are yet unknown, and should be focus of future research.

Supplementary material

Supplementary material is available at *Brain Communications* online.

Acknowledgements

Post-mortem human brain material and CSF were obtained from The Netherlands Brain Bank, Netherlands Institute for Neuroscience (Amsterdam, The Netherlands; open access: www.brainbank.nl). *Ante-mortem* CSF was obtained from UMC Utrecht (Utrecht, The Netherlands), the Ludwig Maximilian University of Munich (Munich, Germany) and Amsterdam UMC (Amsterdam, The Netherlands). The authors acknowledge the HIS Mouse facility of the AMC, Amsterdam, and the Bloemenhove clinic (Heemstede, The Netherlands) for providing foetal tissues.

Funding

This study was funded by Stichting ParkinsonFonds (EMH), Nederlandse Organisatie voor Wetenschappelijk Onderzoek NWO-talentprogramma Vici (NWO VICI) 865.09.003 (EMH), ZonMw Meer Kennis met Minder Dieren (ZonMW MKMD) 11402101 (EMH) and T. & P. Bohnen fund (PAR).

Competing interests

The authors report no competing interests.

References

Adams CW, Abdulla YH, Torres EM, Poston RN. Periventricular lesions in multiple sclerosis: their perivenous origin and relationship to granular ependymitis. Neuropathol Appl Neurobiol 1987; 13: 141–52.

Alonso MI, Lamus F, Carnicero E, Moro JA, de la Mano A, Fernández JMF, et al. Embryonic cerebrospinal fluid increases neurogenic activity in the brain ventricular-subventricular zone of adult mice. Front Neuroanat 2017; 11: 124.

Andersen J, Urbán N, Achimastou A, Ito A, Simic M, Ullom K, et al. A transcriptional mechanism integrating inputs from extracellular signals to activate hippocampal stem cells. Neuron 2014; 83: 1085–97.

Baird GS, Nelson SK, Keeney TR, Stewart A, Williams S, Kraemer S, et al. Age-dependent changes in the cerebrospinal fluid proteome by slow off-rate modified aptamer array. Am J Pathol 2012; 180: 446–56.

Basak O, Giachino C, Fiorini E, Macdonald HR, Taylor V. Neurogenic subventricular zone stem/progenitor cells are Notch1-dependent in their active but not quiescent state. J Neurosci 2012; 32: 5654–66.

Baser A, Skabkin M, Martin-Villalba A. Neural stem cell activation and the role of protein synthesis. Brain Plast 2017; 3: 1–15.

Brandner S, Thaler C, Lelental N, Buchfelder M, Kleindienst A, Maler JM, et al. Ventricular and lumbar cerebrospinal fluid concentrations of Alzheimer's disease biomarkers in patients with normal pressure hydrocephalus and posttraumatic hydrocephalus. J Alzheimers Dis 2014; 41: 1–6.

Buddensiek J, Dressel A, Kowalski M, Runge U, Schroeder H, Hermann A, et al. Cerebrospinal fluid promotes survival and astroglial differentiation of adult human neural progenitor cells but inhibits proliferation and neuronal differentiation. BMC Neurosci 2010; 11: 48.

Buddensiek J, Dressel A, Kowalski M, Storch A, Sabolek M. Adult cerebrospinal fluid inhibits neurogenesis but facilitates gliogenesis from fetal rat neural stem cells. J Neurosci Res 2009; 87: 3054–66.

Chaichana KL, McGirt MJ, Frazier J, Attenello F, Guerrero-Cazares H, Quinones-Hinojosa A. Relationship of glioblastoma multiforme to the lateral ventricles predicts survival following tumor resection. J Neurooncol 2008; 89: 219–24.

Conover JC, Shook B. A. Aging of the subventricular zone neural stem cell niche. Aging Dis 2011; 2: 49–63.

De Filippis L, Lamorte G, Snyder EY, Malgaroli A, Vescovi AL. A novel, immortal, and multipotent human neural stem cell line generating functional neurons and oligodendrocytes. Stem Cells 2007; 25: 2312–21.

Del Bigio MR. Ependymal cells: Biology and pathology. Acta Neuropathol 2010; 119: 55–73.

Doetsch F, Caillé I, Lim DA, García-Verdugo JM, Alvarez-Buylla A. Subventricular zone astrocytes are neural stem cells in the adult mammalian brain. Cell 1999; 97: 703–16.

Domínguez-Pinos MD, Páez P, Jiménez A-J, Weil B, Arráez M-A, Pérez-Fígares J-M, et al. Ependymal denudation and alterations of the subventricular zone occur in human fetuses with a moderate communicating hydrocephalus. J Neuropathol Exp Neurol 2005; 64: 595–604.

Engler A, Rolando C, Giachino C, Saotome I, Erni A, Brien C, et al. Notch2 signaling maintains NSC quiescence in the murine ventricular-subventricular zone. Cell Rep 2018; 22: 992–1002.

Galli R, Binda E, Orfanelli U, Cipelletti B, Gritti A, Vitis SD, et al. Isolation and characterization of tumorigenic, stem-like neural precursors from human glioblastoma isolation and characterization of tumorigenic, stem-like neural precursors from human glioblastoma. Cancer Res 2004; 64: 7011–21.

Gato Á, Moro JA, Alonso MI, Bueno D, De La Mano A, Martín C. Embryonic cerebrospinal fluid regulates neuroepithelial survival, proliferation, and neurogenesis in chick embryos. Anat Rec 2005; 284A: 475–84.

Giese A, Loo MA, Tran N, Haskett D, Coons SW, Berens ME. Dichotomy of astrocytoma migration and proliferation. Int J Cancer 1996; 67: 275–82.

Gómez-Roldán MDC, Pérez-Martín M, Capilla-González V, Cifuentes M, Pérez J, García-Verdugo JM, et al. Neuroblast proliferation on the surface of the adult rat striatal wall after focal ependymal loss by intracerebroventricular injection of neuraminidase. J Comp Neurol 2008; 507: 1571–87.

Gray F, Lescs MC, Keohane C, Paraire F, Marc B, Durigon M, et al. Early brain changes in HIV infection: neuropathological study of 11 HIV seropositive, non-AIDS cases. J Neuropathol Exp Neurol 1992; 51: 177–85.

Honer WG, Bassett AS, Falkai P, Beach TG, Lapointe JS. A case study of temporal lobe development in familial schizophrenia. Psychol Med 1996; 26: 191–5.

Ignatova TN, Kukekov VG, Laywell ED, Suslov ON, Vrionis FD, Steindler DA. Human cortical glial tumors contain neural stem-like cells expressing astroglial and neuronal markers in vitro. Glia 2002; 39: 193–206.

Jackson EL, Alvarez-Buylla A. Characterization of adult neural stem cells and their relation to brain tumors. Cells Tissues Organs 2008; 188: 212–24.

Jackson EL, Garcia-Verdugo JM, Gil-Perotin S, Roy M, Quinones-Hinojosa A, VandenBerg S, et al. PDGFRalpha-positive B cells are neural stem cells in the adult SVZ that form glioma-like growths in response to increased PDGF signaling. Neuron 2006; 51: 187–99.

Jiménez AJ, Domínguez-Pinos M-D, Guerra MM, Fernández-Llebrez P, Pérez-Fígares J-M. Structure and function of the ependymal

barrier and diseases associated with ependyma disruption. Tissue Barriers 2014; 2: e28426.
Jiménez AJ, García-Verdugo JM, Gonzalez CA, Bátiz LF, Rodríguez-Pérez LM, Páez P, et al. Disruption of the neurogenic niche in the subventricular zone of postnatal hydrocephalic hyh mice. J Neuropathol Exp Neurol 2009; 68: 1006–20.
Johansson PA, Cappello S, Götz M. Stem cells niches during development-lessons from the cerebral cortex. Curr Opin Neurobiol 2010; 20: 400–7.
Johnson KP, Johnson RT. Granular ependymitis. Occurrence in myxovirus infected rodents and prevalence in man. Am J Pathol 1972; 67: 511–26.
Kamphuis W, Orre M, Kooijman L, Dahmen M, Hol EM. Differential cell proliferation in the cortex of the appsweps1de9 Alzheimer's disease mouse model. Glia 2012; 60: 615–29.
Kukekov VG, Laywell ED, Suslov O, Davies K, Scheffler B, Thomas LB, et al. Multipotent stem/progenitor cells with similar properties arise from neurogenic regions of adult human brain. Exp Neurol 1999; 156: 333–44.
Kuo CT, Mirzadeh Z, Soriano-Navarro M, Rain M, Wang D, Shen J, et al. Postnatal deletion of Numb/Numblike reveals repair and remodeling capacity in the subventricular neurogenic niche. Cell 2006; 127: 1253–64.
Lantos PL, Pilkington GJ. The development of experimental brain tumours. A sequential light and electron microscope study of the subependymal plate. I. Early lesions (abnormal cell clusters). Acta Neuropathol 1979; 45: 167–75.
Lee JH, Lee JE, Kahng JY, Kim SH, Park JS, Yoon SJ, et al. Human glioblastoma arises from subventricular zone cells with low-level driver mutations. Nature 2018; 560: 243–7.
Lehtinen MK, Walsh C. A. Neurogenesis at the brain-cerebrospinal fluid interface. Annu Rev Cell Dev Biol 2011; 27: 653–79.
Lehtinen MK, Zappaterra MW, Chen X, Yang YJ, Hill AD, Lun M, et al. The cerebrospinal fluid provides a proliferative niche for neural progenitor cells. Neuron 2011; 69: 893–905.
Lim D. A, Cha S, Mayo MC, Chen M-H, Keles E, VandenBerg S, et al. Relationship of glioblastoma multiforme to neural stem cell regions predicts invasive and multifocal tumor phenotype. Neuro Oncol 2007; 9: 424–9.
Luo J, Daniels SB, Lennington JB, Notti RQ, Conover JC. The aging neurogenic subventricular zone. Aging Cell 2006; 5: 139–52.
Luo J, Shook BA, Daniels SB, Conover JC. Subventricular zone-mediated ependyma repair in the adult mammalian brain. J Neurosci 2008; 28: 3804–13.
Ma Y, Liu M, He B. Adult cerebrospinal fluid does not support neurogenesis from fetal rat neural stem cells. Neurol Sci 2013; 34: 735–9.
Middeldorp J, Boer K, Sluijs JA, De Filippis L, Encha-Razavi F, Vescovi AL, et al. GFAPδ in radial glia and subventricular zone progenitors in the developing human cortex. Development 2010; 137: 313–21.
Mirzadeh Z, Merkle FT, Soriano-Navarro M, Garcia-Verdugo JM, Alvarez-Buylla A. Neural stem cells confer unique pinwheel architecture to the ventricular surface in neurogenic regions of the adult brain. Cell Stem Cell 2008; 3: 265–78.
Muthusamy N, Sommerville LJ, Moeser AJ, Stumpo DJ, Sannes P, Adler K, et al. MARCKS-dependent mucin clearance and lipid metabolism in ependymal cells are required for maintenance of forebrain homeostasis during aging. Aging Cell 2015; 14: 764–73.
Netherlands Brain Bank [Internet]. 2020. Amsterdam: Netherlands Institute for Neuroscience [cited 23 January 2020]. Available from: https://www.brainbank.nl.
Nielsen S, Arnulf Nagelhus E, Amiry-Moghaddam M, Bourque C, Agre P, Petter Ottersen O. Specialized membrane domains for water transport in glial cells. J Neurosci 1997; 17: 171–80.
Oreković D, Klarica M. The formation of cerebrospinal fluid: nearly a hundred years of interpretations and misinterpretations. Brain Res Rev 2010; 64: 241–62.
Ortega JA, Memi F, Radonjic N, Filipovic R, Bagasrawala I, Zecevic N, et al. The subventricular zone: a key player in human neocortical development. Neuroscientist 2018; 24: 156–70.
Quiñones-Hinojosa A, Chaichana K. The human subventricular zone: a source of new cells and a potential source of brain tumors. Exp Neurol 2007; 205: 313–24.
Rasband WI. [Software]. U. S. National Institutes of Health. Bethesda, Maryland, USA 2015. http://imagej.nih.gov/ij/.
Roales-Buján R, Páez P, Guerra M, Rodríguez S, Vío K, Ho-Plagaro A, et al. Astrocytes acquire morphological and functional characteristics of ependymal cells following disruption of ependyma in hydrocephalus. Acta Neuropathol 2012; 124: 531–46.
Roelofs RF, Fischer DF, Houtman SH, Sluijs JA, Van Haren W, Van Leeuwen FW, et al. Adult human subventricular, subgranular, and subpial zones contain astrocytes with a specialized intermediate filament cytoskeleton. Glia 2005; 52: 289–300.
Sanai N, Alvarez-Buylla A, Berger MS. Neural stem cells and the origin of gliomas. N Engl J Med 2005; 353: 811–22.
Sanai N, Nguyen T, Ihrie RA, Mirzadeh Z, Tsai H-H, Wong M, et al. Corridors of migrating neurons in the human brain and their decline during infancy. Nature 2011; 478: 382–6.
Sanai N, Tramontin AD, Quiñones-Hinojosa A, Barbaro NM, Gupta N, Kunwar S, et al. Unique astrocyte ribbon in adult human brain contains neural stem cells but lacks chain migration. Nature 2004; 427: 740–4.
Sarnat HB. Ependymal reactions to injury. A review. J Neuropathol Exp Neurol 1995; 54: 1–15.
Sawamoto K. New neurons follow the flow of cerebrospinal fluid in the adult brain. Science. 2006; 311: 629–32.
Schauer R. Sialic acids as regulators of molecular and cellular interactions. Curr Opin Struct Biol 2009; 19: 507–14.
Schwarz N, Hedrich UBS, Schwarz H, Harshad PA, Dammeier N, Auffenberg E, et al. Human cerebrospinal fluid promotes long-term neuronal viability and network function in human neocortical organotypic brain slice cultures. Sci Rep 2017; 7: 12249.
Silva-Vargas V, Maldonado-Soto AR, Mizrak D, Codega P, Doetsch F. Age-dependent niche signals from the choroid plexus regulate adult neural stem cells. Cell Stem Cell 2016; 19: 643–52.
Singh SK, Hawkins C, Clarke ID, Squire JA, Bayani J, Hide T, et al. Identification of human brain tumour initiating cells. Nature 2004; 432: 396–401.
Sommer JB, Gaul C, Heckmann J, Neundörfer B, Erbguth FJ. Does lumbar cerebrospinal fluid reflect ventricular cerebrospinal fluid? A prospective study in patients with external ventricular drainage. Eur Neurol 2002; 47: 224–32.
Spassky N. Adult ependymal cells are postmitotic and are derived from radial glial cells during embryogenesis. J Neurosci 2005; 25: 10–8.
Steed TC, Treiber JM, Patel K, Ramakrishnan V, Merk A, Smith AR, et al. Differential localization of glioblastoma subtype: implications on glioblastoma pathogenesis. Oncotarget 2016; 7: 24899–907.
van den Berge SA, Middeldorp J, Zhang CE, Curtis MA, Leonard BW, Mastroeni D, et al. Longterm quiescent cells in the aged human subventricular neurogenic system specifically express GFAP-δ. Aging Cell 2010; 9: 313–26.
van den Berge SA, van Strien ME, Korecka JA, Dijkstra AA, Sluijs JA, Kooijman L, et al. The proliferative capacity of the subventricular zone is maintained in the parkinsonian brain. Brain 2011; 134: 3249–63.
Van Dijk KD, Bidinosti M, Weiss A, Raijmakers P, Berendse HW, van de Berg WDJ. Reduced α-synuclein levels in cerebrospinal fluid in Parkinson's disease are unrelated to clinical and imaging measures of disease severity. Eur J Neurol 2014; 21: 388–94.
Van Dijk KD, Persichetti E, Chiasserini D, Eusebi P, Beccari T, Calabresi P, et al. Changes in endolysosomal enzyme activities in cerebrospinal

fluid of patients with Parkinson's disease. Mov Disord 2013; 28: 747–54.
van Strien ME, van den Berge SA, Hol EM. Migrating neuroblasts in the adult human brain: a stream reduced to a trickle. Cell Res 2011; 21: 1523–5.
van Strien ME, Sluijs JA, Reynolds BA, Steindler DA, Aronica E, Hol EM. Isolation of neural progenitor cells from the human adult subventricular zone based on expression of the cell surface marker CD271. Stem Cells Transl Med 2014; 3: 470–80.
Veening JG, Barendregt HP. The regulation of brain states by neuroactive substances distributed via the cerebrospinal fluid; a review. Cerebrospinal Fluid Res 2010; 7: 1.
Whish S, Dziegielewska KM, Mã¸llgÃ¥Rd K, Noor NM, Liddelow SA, Habgood MD, et al. The inner CSF-brain barrier: developmentally controlled access to the brain via intercellular junctions. Front Neurosci 2015; 9: 1–15.
Zappaterra MW, Lehtinen MK. The cerebrospinal fluid: regulator of neurogenesis, behavior, and beyond. Cell Mol Life Sci 2012; 69: 2863–78.
Zhang J, Goodlett DR, Peskind ER, Quinn JF, Zhou Y, Wang Q, et al. Quantitative proteomic analysis of age-related changes in human cerebrospinal fluid. Neurobiol Aging 2005; 26: 207–27.
Zhang J, Piontek J, Wolburg H, Piehl C, Liss M, Otten C, et al. Establishment of a neuroepithelial barrier by Claudin5a is essential for zebrafish brain ventricular lumen expansion. Proc Natl Acad Sci USA 2010; 107: 1425–30.
Zhu M, Feng Y, Dangelmajer S, Guerrero-Cazares H, Chaichana KL, Smith CL, et al. Human cerebrospinal fluid regulates proliferation and migration of stem cells through insulin-like growth factor-1. Stem Cells Dev 2015; 24: 160–71.
Zhu Y, Guignard F, Zhao D, Liu L, Burns DK, Mason RP, et al. Early inactivation of p53 tumor suppressor gene cooperating with NF1 loss induces malignant astrocytoma. Cancer Cell 2005; 8: 119–30.